


Hepatotoxic Dose Thresholds by Positron-Emission Tomography After Yttrium-90 Radioembolization of Liver Tumors: A Prospective Single-Arm Observational Study

Keith T. Chan¹ · Adam M. Alessio² · Guy E. Johnson¹ · Sandeep Vaidya¹ · Sharon W. Kwan¹ · Wayne Monsky¹ · Ann E. Wilson² · David H. Lewis³ · Siddharth A. Padia⁴ 

Received: 28 November 2017 / Accepted: 27 March 2018 / Published online: 12 April 2018

© Springer Science+Business Media, LLC, part of Springer Nature and the Cardiovascular and Interventional Radiological Society of Europe (CIRSE) 2018

Abstract

Purpose To define a threshold radiation dose to non-tumoral liver from ⁹⁰Y radioembolization that results in hepatic toxicity using pair-production PET.

Materials and Methods This prospective single-arm study enrolled 35 patients undergoing radioembolization. A total of 34 patients (27 with HCC and 7 with liver metastases) were included in the final analysis. Of 27 patients with underlying cirrhosis, 22 and 5 patients were Child–Pugh A and B, respectively. Glass and resin microspheres were used in 32 (94%) and 2 (6%) patients, respectively. Lobar and segmental treatment was done in 26 (76%) and 8 (24%) patients, respectively. Volumetric analysis was performed on post-radioembolization time-of-flight PET imaging to determine non-tumoral parenchymal dose. Hepatic toxicity was evaluated up to 120 days post-treatment, with CTCAE grade ≤ 1 compared to grade ≥ 2 .

Results The median dose delivered to the non-tumoral liver in the treated lobe was 49 Gy (range 0–133). A total

of 15 patients had grade ≤ 1 hepatic toxicity, and 19 patients had grade ≥ 2 toxicity. Patients with a grade ≥ 2 change in composite toxicity (70.7 vs. 43.8 Gy), bilirubin (74.1 vs. 43.3 Gy), albumin (84.2 vs. 43.8 Gy), and AST (94.5 vs. 47.1 Gy) have significantly higher non-tumoral parenchymal doses than those with grade ≤ 1 . Liver parenchymal dose and Child–Pugh status predicted grade ≥ 2 toxicity, observed above a dose threshold of 54 Gy.

Conclusion Increasing delivered ⁹⁰Y dose to non-tumoral liver measured by internal pair-production PET correlates with post-treatment hepatic toxicity. The likelihood of toxicity exceeds 50% at a dose threshold of 54 Gy.

ClinicalTrials.gov identifier: NCT02848638.

Keywords Radioembolization · Yttrium-90 · PET · Hepatocellular carcinoma · Dosimetry

✉ Siddharth A. Padia
spadia@gmail.com

¹ Division of Interventional Radiology, Department of Radiology, University of Washington, 1959 NE Pacific St., Box 357115, Seattle, WA 98195-7115, USA

² Department of Radiology, University of Washington, 1959 NE Pacific St., Box 357115, Seattle, WA 98195-7115, USA

³ Division of Nuclear Medicine, Department of Radiology, Harborview Medical Center, 325 9th Ave, Seattle, WA 98104, USA

⁴ Division of Interventional Radiology, Department of Radiology, David Geffen School of Medicine at University of California Los Angeles, 757 Westwood Plaza, Suite 2125, Los Angeles, CA 90095-7430, USA

Introduction

Yttrium-90 (⁹⁰Y) radioembolization allows delivery of high radiation doses to hypervascular tumors compared to surrounding liver parenchyma, due to preferential uptake of microspheres by tumors [1]. Multiple studies suggest a tumor dose–response relationship to ⁹⁰Y radioembolization, with longer progression-free and overall survival when hepatic tumors receive increasing doses [2, 3]. However, increasing delivered radiation dose may also result in excessive radiation to the non-tumoral hepatic parenchyma and increased rates of liver toxicity [4] and can result in a range of sequela from transient effects such

as elevation in AST/ALT and hyperbilirubinemia to ascites, irreversible fibrosis and liver failure [1, 5, 6]. A wide range of acceptable radiation dose limits from 30 to 390 Gy to the non-tumoral liver parenchyma has been proposed before permanent damage occurs [7–11].

The ideal radioembolization dose maximizes treatment effectiveness and minimizes toxicity. However, treatment planning is further complicated by the difficulty in measuring the actual delivered ^{90}Y radiation dose [12]. Current dose calculations do not account for variations in tumor hypervascularity, preferential uptake by tumor versus the normal liver, non-uniform particle distribution, diminished vasculature from prior treatment, or arteriportal shunting.

Post-treatment ^{90}Y internal pair-production positron-emission tomography (PET) imaging is a recent dose quantification technique with higher accuracy and spatial resolution than pre-treatment $^{99\text{m}}\text{Tc}$ -MAA SPECT and post-treatment ^{90}Y bremsstrahlung SPECT [13, 14]. This technique allows the actual non-tumoral parenchymal dose to be measured.

The purpose of this study is to evaluate the use of ^{90}Y PET dosimetry to quantify the radiation dose in non-tumoral liver after radioembolization and identify a dose threshold for treatment-related liver toxicity.

Materials and Methods

Patient Selection

A prospective single-arm observational study was performed at a single academic hospital with institutional review board approval. Eligible patients were identified among those referred from the institution's multidisciplinary liver tumor board from 2012 to 2014 for ^{90}Y radioembolization to treat unresectable hepatocellular carcinoma (HCC) or non-HCC intrahepatic malignancies. Patients who qualified for surgical resection, thermal ablation, or expected liver transplantation within 3 months were excluded. Patients who are not candidates for these treatments due to portal hypertension, comorbidities and surgical risk, tumor size > 3 cm or tumor proximity to the portal vein were then referred for radioembolization. Patients selected met the following inclusion criteria: Barcelona Clinic Liver Cancer (BCLC) stage A–C hepatocellular carcinoma, Eastern Cooperative Oncology Group (ECOG) performance score of 0–2, and liver function compatible with treatment (non-cirrhotic, or cirrhosis with Childs–Pugh A or B). Patients with secondary liver malignancies have unresectable liver-dominant metastatic disease and failed standard chemotherapy before being referred for ^{90}Y locoregional control. Patients with prior liver radioembolization or transarterial chemoembolization

were also excluded. Systemic chemotherapy was stopped at least 4 weeks prior to radioembolization; chemotherapy may resume 1 month after treatment. Informed consent was obtained from each patient at the time of screening. Institutional HIPAA practices were employed.

During the study period, a total of 210 patients underwent radioembolization, from which 35 patients were enrolled in the study. The most common causes for not enrolling in the study were prior radioembolization or chemoembolization, lack of PET scanner availability on day of ^{90}Y treatment, and patient refusal for post-treatment transportation to a separate medical center for PET imaging. One patient in the enrolled cohort was excluded from analysis due to technical reasons on the post-treatment PET imaging that prevented dosimetry calculation. Of the 34 remaining patients, 27 patients (79%) had HCC and 7 patients (21%) had non-HCC malignancies.

Baseline patient demographics for the 34 subjects are shown in Table 1, which represents 52 treated tumors (38 HCC and 14 non-HCC, with 9 colorectal carcinoma, 1 cholangiocarcinoma, 3 mucoepidermoid carcinoma, and 1

Table 1 Baseline patient demographics

Number of patients	34
Age at treatment, median [range]	61.0 years [45.6–79.0 years]
% Male	26/34 (76%)
ECOG status 0	24/34 (71%)
ECOG status ≥ 1	8/34 (29%)
Tumor diameter, median [range]	5.5 cm [2.8–17.9 cm]
Hepatocellular carcinoma ($n = 27$)	
Degree of cirrhosis and staging	
Childs–Pugh A	22/27 (81%)
Childs–Pugh B	5/27 (19%)
BCLC stage A	7/27 (26%)
BCLC stage B	7/27 (26%)
BCLC stage C	13/27 (48%)
Multifocal disease	12/27 (44%)
Portal vein invasion	
None	14/27 (52%)
Segmental or lobar	11/27 (41%)
Main portal	2/27 (7%)
Tumor burden, % of liver volume	
1–25%	19/27 (70%)
25–50%	8/27 (30%)
Hepatic metastases ($n = 7$)	
Colorectal cancer	3/7 (43%)
Cholangiocarcinoma	1/7 (14%)
Neuroendocrine	1/7 (14%)
Ocular melanoma	1/7 (14%)
Mucoepidermoid carcinoma	1/7 (14%)

ocular melanoma). 18 patients (53%) had multifocal disease. Patients with non-HCC malignancies had bilobar disease with less than 25% total liver involvement but no prior history of liver disease; their liver function tests were all normal prior to radioembolization. All 27 HCC patients had a diagnosis of cirrhosis by imaging; the predominant risk factors for cirrhosis were HBV/HCV infection in 22 patients (81%) and alcohol use in 8 patients (30%). Among the 27 HCC patients, 22 (81%) and 5 (19%) were Child–Pugh class A and B, respectively. Pre-treatment liver dysfunction was characterized with labs obtained the morning of treatment, with 6 (22%) having baseline grade 2 hypoalbuminemia (2.0–2.9 g/dL), 1 (4%) with grade 2 hyperbilirubinemia (2.0–3.9 g/dL), 1 (4%) with grade 2 (120–200 u/L) and 3 (11%) with grade 3 (200–800 u/L) abnormal AST, 4 (15%) with grade 2 (144–240 u/L) abnormal ALT, and 2 (7%) grade 2 (2.0–3.0 k/mL) and 1 (4%) grade 3 (1.0–2.0 k/mL) leukopenia. Eighteen of the 27 (67%) of the HCC patients had tumor burden of less than 25% of the total liver volume, and the remainder had tumor involving 26–50% of the total liver volume.

Radioembolization

Baseline contrast-enhanced CT or MR liver imaging was performed within 30 days of the mapping angiogram. Radioembolization was performed according to standard practice [15, 16], including a mapping angiogram and lung shunt fraction determination. Pre-treatment coil embolization of extrahepatic arteries was performed at the discretion of the interventional radiologist.

The decision to use glass (TheraSphere, BTG, Ottawa, Canada) or resin (SirSphere, Sirtex, Australia) ^{90}Y microspheres was based on the interventional radiologist's preference. For glass microspheres, dosimetry was based on the MIRD model with a target dose of 120 Gy for lobar treatments, and higher doses were permitted for segmental treatments [17]. For resin microsphere activity calculations, a body-surface area calculation was used, according to the manufacturer's instructions. ^{90}Y treatment was then performed at a median of 12 days (range 3–28 days) after the mapping angiogram by one of four board-certified Interventional Radiologists with 3–11 years of experience. No treatment was repeated during the follow-up period.

Post-treatment Evaluation

Following treatment, a time-of-flight ^{90}Y PET/CT (Gemini TF64; Philips Healthcare) was performed on the same day without the use of any additional intravenous radiotracer (e.g. FDG) since ^{90}Y energy leads to positron–electron pair production in tissue [3]. Scan parameters included 12-min 144×144 pixels acquisitions with 4-mm isotropic

resolution over two PET bed positions and standard algorithms and scatter/attenuation corrections. Adjustments for ^{90}Y were performed based on ^{18}F decays and differences in positron fraction (3.19×10^{-5} per decay versus 9.2×10^{-1} for ^{18}F), allowing conversion from apparent Bq/cc to ^{90}Y activity concentration. The correction used for our acquisitions was $28,210 * [^{90}\text{Y} \text{ Bq}] / [\text{apparent } ^{18}\text{F} \text{ Bq}]$. For attenuation correction, non-contrast CT imaging was obtained using settings of 120 kVp, 50 mA, 0.75-second rotation, and pitch of 0.7:1.

^{90}Y PET dosimetry was calculated using a commercial image analysis software (Imalytics, Philips Technologie GmbH, Innovative Technologies, Aachen, Germany) on a 3D workstation. Volumes of interest corresponding to the anatomic margins of the treated tumors and surrounding non-tumoral liver lobe (entire right or left liver lobar volume, ipsilateral to the treated arterial distribution, *excluding* the tumors) were selected (Fig. 1) using the pre-treatment multiphase CT or MR by a single board-certified radiologist with 1 year of experience who was blinded to the primary outcome and the ^{90}Y treatment [18]. The number of coincident events was assessed for each voxel across the volumes of interest, allowing for a ^{90}Y dose and a dose-volume histogram to be calculated based on a pre-calibrated conversion factor. The median delivered dose and median volume of the non-tumoral liver lobe were recorded.

Patient Follow-Up

Primary outcomes included clinical and laboratory assessment at 1 and 4 months after treatment. No patient was lost to follow-up during this observational period. The optimal duration for assessing radiation-induced liver disease is described to be within 4 months of treatment, with longer-term observations confounded by the natural progression of underlying liver cirrhosis [19]. Longer-term follow-up (until transplant or death) was continued after study completion as part of routine clinical care. Serum bilirubin, albumin, leukocyte count, aspartate aminotransferase (AST) and alanine aminotransferase (ALT) levels were tested and categorized in accordance with the National Institute of Health's Common Terminology Criteria for Adverse Events (CTCAE) definitions [20]. In patients with liver dysfunction at baseline, toxicity was only counted if laboratory values worsened by at least one CTCAE grade during the follow-up period [21]. Significant toxicity was defined by progression to grade 2 or higher as this would affect eligibility for future treatment.

Statistical Analysis and Sample Size Calculation

Statistical analysis was performed using JMP version 9 software (SAS Institute, Inc., Cary, NC). Kruskal–Wallis

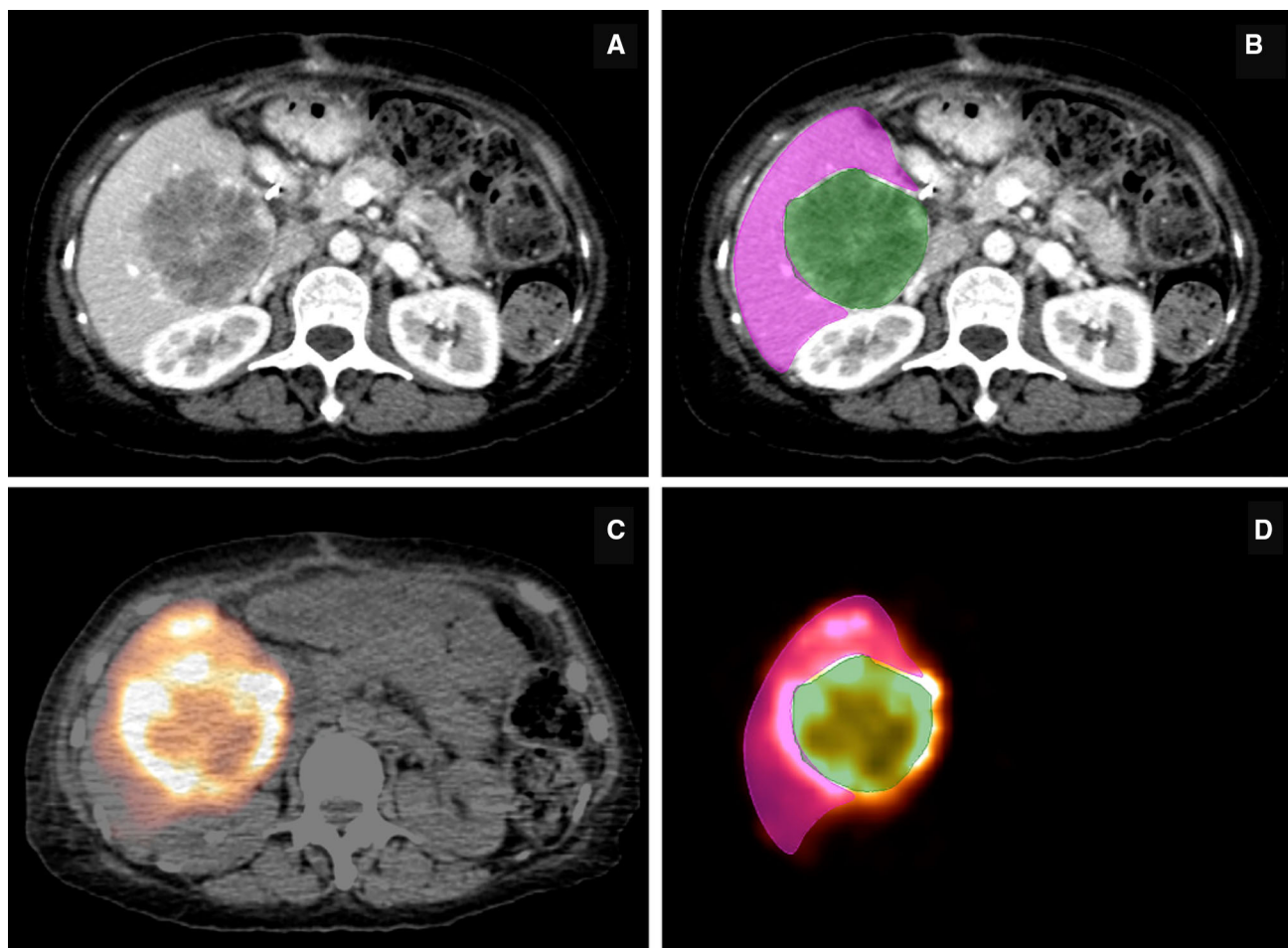


Fig. 1 **A** 65 year old with a large partially necrotic hepatocellular carcinoma in segment 5/6. **B** Volumes of interest were superimposed on baseline contrast-enhanced CT delineating tumor (green) from normal liver (pink). **C** Lobar radioembolization was performed using glass microspheres, with post-radioembolization PET fused with

baseline CT showing heterogeneous microsphere distribution within the tumor and the surrounding parenchyma. **D** Volumes of interest corresponding with ^{90}Y distribution. In this case, the dose to the normal liver parenchyma was 69 Gy and the dose to the tumor was 268 Gy

nonparametric testing was performed to assess for the effects between grade ≥ 2 toxicity (composite of all 5 individual toxicities, and each individual toxicity) and non-tumoral liver dose and volume, baseline patient and treatment characteristics including Child–Pugh status, HCC versus non-HCC malignancy, and lobar versus segmental arterial infusion. Testing for the primary effect of glass versus resin microspheres was not performed due to the inadequate number of resin treatments for a meaningful analysis; however, Cochran–Mantel–Haenszel testing was performed to assess for interactions between type of malignancy and glass versus resin microsphere and Child–Pugh status and segmental versus lobar treatment. Using the significant factors identified by univariate analysis, multiple regression modeling was performed to evaluate for composite and individual grade ≥ 2 toxicities. Two-tailed p value < 0.05 was considered significant.

Predicted toxicity at incrementally increasing non-tumoral liver doses was calculated using a multiple

regression model. Since higher proportions of toxicity grades continuously increased with radiation dose, the thresholds of 50, 75, and 100 Gy were chosen to represent possible delivered non-tumoral liver doses in practical situations. Finally, multiple regression predictive modeling was performed to determine the liver dose needed for 50% likelihood or greater of a grade 2/3 toxicity (D_{50}).

Laboratory toxicity has been described in 30–40% of patients treated with radioembolization [22, 23], but no “dose-escalation” literature exists for the likelihood of toxicity with varying levels of radiation. Using an expected 30% toxicity incidence, we hypothesized our study population will dichotomize into two exposure levels—patients who receive “low” versus “high” radiation doses are arbitrarily assigned a halved (15%) or doubled (60%) likelihood of toxicity, respectively. Assuming an equal number of patients in each group, a total sample size of 38 was required to demonstrate a difference between the

groups with two-sided significance level < 0.05 and 0.80 power. While initial budgeting was designed for this study size, unforeseen increases in the costs of study execution resulted in a total enrollment of 35 subjects.

The design and execution of the study, analysis of data, and manuscript preparation were performed solely by the authors without involvement or conditions by the sponsor.

Results

Treatment Parameters

All ^{90}Y treatments were technically successful. Thirty-two (94%) patients were treated with glass microspheres, and two patients (6%, both with non-HCC malignancies) received resin microspheres. Lobar treatment was performed in 26 patients (76%) and segmental treatment in 8 patients (24%). The median administered activity was 2.7 GBq (range 0.3–9.5 GBq). Median non-tumoral liver dose was 49.4 Gy (range 0–133 Gy), and median treated non-tumoral liver volume was 1065 cc (range 88–2041 cc). The median non-tumoral liver volumes represented 89% of the entire liver lobe (range 3–97%). The dose to the treated non-tumoral liver was not correlated with the liver volume ($r^2 = 0.06$) or injected activity ($r^2 = 0.08$). The median liver dose was higher for treatments by lobar arterial distribution (64.3 Gy, range 6–133 Gy) than by segmental arterial distribution (40.8 Gy, range 1–50 Gy, $p = 0.046$).

Toxicity Assessment

The median duration of follow-up was 684 days. Common post-radioembolization toxicities included 9 patients with fatigue (26%), 7 patients (21%) with moderate or greater abdominal pain, and 5 patients (15%) with post-embolization syndrome. A total of 19 patients (56%) developed at least one grade 2 or 3 laboratory toxicity (Table 2). No patients had grade 4 or 5 toxicities. Two patients developed irreversible ascites during the follow-up period: one patient (who received 84 Gy to the liver lobe) progressed to Child–Pugh C status therefore limiting additional treatments; the other patient developed ascites from worsening metastatic disease. No biloma, abscess, encephalopathy, liver failure, extrahepatic complication or patient death occurred during the 4-month study period.

Univariate Analysis

Patients with composite grade 2 or higher laboratory toxicity (Table 2), when compared with those without any toxicity, had a significantly higher median non-tumoral

liver dose (70.7 vs. 43.8 Gy, $p = 0.02$), were more likely to be Child–Pugh class B than A (RR = 2.07, $p = 0.03$), and had lobar instead of segmental arterial infusions (RR = 2.62, $p = 0.04$). Factors not significant for grade 2 or higher toxicity included the volume of the treated non-tumoral liver ($p = 0.14$), volume of the untreated liver volume ($p = 0.36$), presence of portal venous tumor or thrombus ($p = 0.27$), type of malignancy ($p = 0.44$), and whether the tumors involved $\leq 25\%$ or 26–50% of the liver ($p = 0.76$).

Patients with grade 2 or higher change in post-treatment albumin (74.1 vs. 43.3 Gy, $p = 0.013$), bilirubin (84.2 vs. 43.8 Gy, $p < 0.001$), and AST (94.5 vs. 47.1 Gy, $p = 0.048$) received higher non-tumoral liver doses compared to patients without laboratory toxicity (Fig. 2). Non-tumoral liver dose was not statistically higher for patients that exhibited grade 2 or higher change in ALT or leukopenia. Median non-tumoral liver doses for the composite and individual toxicities are shown in Table 3.

Compared to patients with HCC and cirrhosis, all 7 patients with non-HCC malignancy had normal liver function and pre-treatment biochemical values. Subgroup analysis using Pearson's likelihood ratio did not reveal a correlation between those with or without cirrhosis and the development of grade 2 or higher toxicity (16/27 or 59% vs. 3/7 or 43%, $p = 0.44$). The median non-tumoral liver doses were higher for HCC than non-HCC patients, but this difference was not statistically significant (51.0 vs. 36.9 Gy, $p = 0.15$).

No interaction was found using Cochran–Mantel–Haenszel testing between the type of malignancy and glass versus resin microsphere ($p = 0.43$), or Child–Pugh status and segmental versus lobar treatment ($p = 0.17$). The delivered median liver dose among those with Child–Pugh A and B were similar (49.5 vs. 44.9 Gy, $p = 0.86$).

Multivariate Analysis

Individual multiple regression models were used to predict grade 2 or higher post-treatment toxicities (Table 4). When accounting for multiple risk factors, non-tumoral liver dose was a significant predictive factor for composite toxicity, hyperbilirubinemia, and AST elevation. Each 1 Gy increase in non-tumoral liver dose increased the odds of composite toxicity, hypoalbuminemia, hyperbilirubinemia and AST elevation by 1.05, 1.08, and 1.39, respectively. Within these multiple regression models, Child–Pugh class B was associated with composite toxicity, hypoalbuminemia, and AST elevation. The volume of the untreated liver had a significant effect on AST elevation, and only treatment by lobar infusion significantly affected ALT elevation. None of these factors predicted post-treatment leukopenia.

Table 2 Post-treatment liver toxicities by common terminology criteria for adverse events (CTCAE) category

	Grade 0/1	Grade 2/3	<i>p</i> value
Incidence of composite of any grade ≥ 2 toxicity	15/34 (44%)	19/34 (56%)	–
Incidence of individual toxicities			
Hypoalbuminemia	21/34 (62%)	13/34 (38%)	–
Hyperbilirubinemia	27/34 (79%)	7/34 (21%)	–
Aspartate aminotransferase (AST) increase	32/34 (94%)	2/34 (6%)	–
Alanine aminotransferase (ALT) increase	25/34 (74%)	9/34 (26%)	–
Leukopenia	28/34 (82%)	6/34 (18%)	–
Univariate analysis of risk factors for composite grade ≥ 2 toxicity			
Non-tumoral liver dose	–†	–†	0.02*
Non-tumoral liver volume	–†	–†	0.14
Untreated liver volume	–†	–†	0.36
Pre-treatment Child–Pugh class			
A	15/29 (52%)	14/29 (48%)	0.03*
B	0/0 (0%)	5/5 (100%)	
Portal venous tumor or thrombus			
No	10/20 (50%)	10/20 (50%)	0.27
Yes	4/13 (31%)	9/13 (69%)	
Arterial infusion			
Segmental	6/8 (75%)	2/8 (25%)	0.04*
Lobar	9/26 (35%)	17/26 (65%)	
Tumor type			
Hepatocellular carcinoma	11/27 (41%)	16/27 (59%)	0.44
Non-HCC liver metastases	4/7 (57%)	3/7 (43%)	
Tumor burden, % of liver involvement			
1–25%	11/24 (46%)	13/24 (54%)	0.76
26–50%	4/10 (40%)	6/10 (60%)	

Factors that meet statistical significance ($p = 0.05$) indicated by asterisk. Non-tumoral liver dose and volume are continuous variables, denoted by †

Predictions for composite toxicity at incrementally increasing non-tumoral liver doses were calculated using the multiple regression model (Table 5). The likelihood of composite toxicity with radiation dose, with a greater likelihood of grade 0/1 toxicity at a liver dose of 50 Gy, versus a high likelihood of grade 2/3 toxicity when 75 or 100 Gy was received. Using these multivariate models, the D_{50} for composite toxicity was 54.2 Gy.

To assess for interaction between lobar versus segmental treatment and the effect of dose on liver toxicity, a post hoc subgroup multivariate analysis was performed including only patients with either lobar or segmental treatments. Similar to our primary analysis based on all 34 subjects, in the lobar treatments, the parenchymal dose was the only statistically significant factor ($p = 0.015$), but pre-existing toxicity or Child–Pugh did not meet significance; a subgroup analysis without the segmentally treated patients did not change the study conclusion. In contrast, the model with segmental-only treatment did not find any of the

variables to be significant for toxicity—also, the median lobar parenchymal dose received only ranged from 0.2 to 22 Gy. (The treated segment was as high as 631 Gy.) This confirms the findings from the primary analysis, showing a low lobar radiation dose is not associated with toxicity.

Discussion

Despite significant advancements in radioembolization practices over the past decade, dosimetry has remained based on standardized models, with dose adjustments empirically made at the physician's discretion based subjectively on concerns of underlying liver function and size of the treatment territory [24]. Maximum non-tumor liver doses of 50–70 Gy or even lower have also been proposed based on partition modeling dosimetry [25]. These proposed dose limits were arbitrarily set without an accurate method to assess dose deposition after radioembolization,

Fig. 2 Box-and-whisker plots of delivered ⁹⁰Y doses to non-tumoral liver parenchyma of the treated lobe versus CTCAE categories of liver toxicity. Statistically significant differences (*p* < 0.05) marked by asterisk

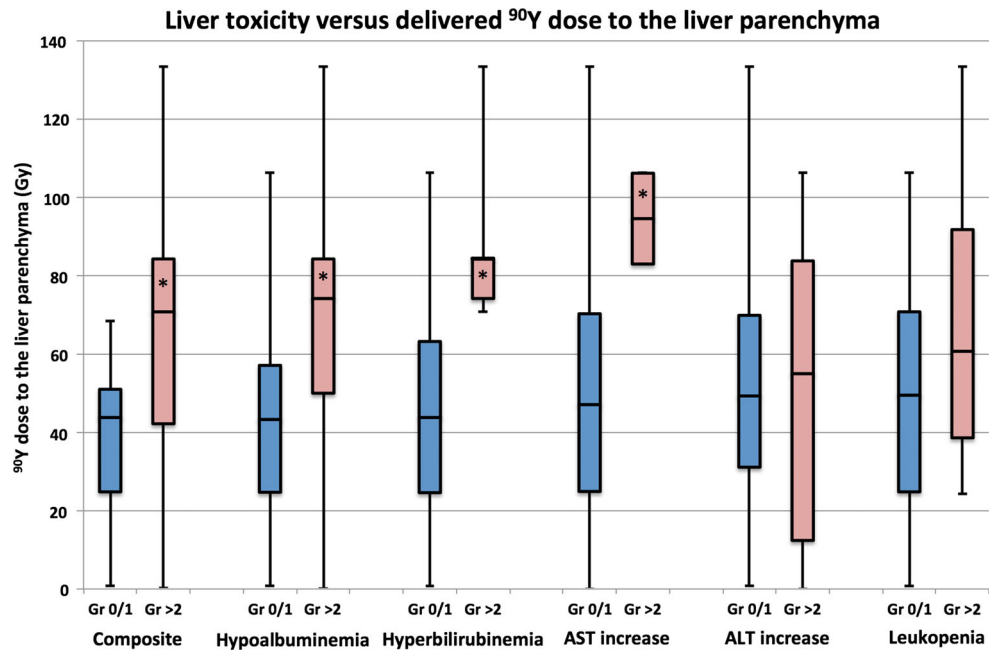


Table 3 Non-tumoral liver doses by toxicities after ⁹⁰Y radioembolization

	Composite (any toxicity)	Individual laboratory toxicities				
		Hypoalbuminemia	Hyperbilirubinemia	AST increase	ALT increase	Leukopenia
Dose to non-tumoral liver volume, median Gy [range]						
No change or grade 1	43.8 [1–68]	43.3 [1–106]	43.8 [0–106]	47.1 [0–133]	49.3 [1–133]	49.5 [0–106]
Grade 2 or higher	70.7 [0–133]	74.1 [0–133]	84.2 [71–133]	94.5 [83–106]	55.0 [0–106]	60.7 [24–133]
Univariate model <i>p</i> value	0.02*	0.01*	< 0.01*	0.05*	0.86	0.44

Factors that meet statistical significance (*p* = 0.05) indicated by asterisk

Table 4 Multivariate models predicting toxicity (CTCAE) after ⁹⁰Y radioembolization

	Composite (any toxicity)	Individual laboratory toxicities				
		Hypoalbuminemia	Hyperbilirubinemia	AST increase	ALT increase	Leukopenia
Multivariate model factors (<i>p</i> values)						
Dose to treated lobe	0.03*	0.16	0.01*	< 0.01*	0.23	0.28
Volume of treated lobe	< 0.01*	0.76	0.25	1.00	0.25	0.16
Volume of untreated lobe	0.45	0.67	0.51	0.04*	0.25	0.55
Childs–Pugh grade B	< 0.01*	< 0.01*	0.65	< 0.01*	0.96	0.12
Portal vein tumor	0.83	0.55	< 0.01*	1.00	0.25	0.69
Lobar treatment	0.36	0.33	0.99	1.00	0.01*	0.25

Factors that meet statistical significance (*p* = 0.05) indicated by asterisk

and prospective correlation with toxicity has not been made. The thresholds and toxicity data reported in most

existing studies are also based on the administered activity for resin microspheres or presumed delivered dose for glass

Table 5 Likelihood of liver toxicities by radiation dose

Composite toxicity by liver dose (Gy)	Grade 0/1 (%)	Grade 2/3 (%)
50	58	42
75	16	84
100	2	98

microspheres. These formulas assume a uniform distribution of microspheres and may not reflect the actual ^{90}Y distribution across the non-tumoral hepatic parenchyma and to the tumors. Knowledge of threshold dose to induce liver toxicity is vital to improving outcomes from radioembolization.

This study found that increasing delivered radiation dose to the non-tumoral liver parenchyma, calculated using post-treatment ^{90}Y pair-production PET, is correlated with liver toxicity manifested by grade 2 (or greater) alterations in a composite of any toxicity, and individual laboratory changes in bilirubin and AST [21, 26, 27]. ^{90}Y PET quantitative dosimetry allows for precise assessment of the actual delivered dose to both tumor and surrounding parenchyma [13, 14]. Even though ^{90}Y PET is obtained after treatment has already been completed, assessment of dose to the hepatic parenchyma could help predict toxicity in those patients who received excessive radiation dose to the normal liver. Debates continue on the safety of repeat radioembolization in patients, with limited evidence to support safety with successive treatments [28]. In those patients who received minimal dose to the normal liver as determined by PET, repeat radioembolization treatments in the setting of disease progression may theoretically be safe. Our findings reflect treatments that are lobar or segmental; the resultant toxicity may be different if a whole-liver treatment was performed.

Post-radioembolization toxicity is believed to be associated with the volume of liver treated and available hepatic reserve [29]. This equates to a presumed higher risk of toxicity for patients with Child–Pugh B status and those who receive treatment to larger areas of liver via a lobar artery administration. We found that Child–Pugh status was a significant predictor of toxicity in 3 of the 6 multivariate models. Similarly, the dose to the liver parenchyma was also found to be a common significant factor in 3 of 6 multiple regression models when accounting for these other variables. These findings suggest that while lobar arterial infusion or the volume of treated liver may increase the risk of specific laboratory toxicities, the strongest predictors of a patient having any post-treatment toxicity are the liver parenchymal dose and Child–Pugh status.

The study's multiple regression models predicted a D_{50} threshold for composite grade 2 change of 54.2 Gy, which is remarkably similar to the D_{50} of 52 Gy previously described for grade ≥ 2 toxicities in a similar patient

population using bremsstrahlung SPECT [22]. For a median liver parenchymal dose of 50 Gy, this model predicts patients would likely have grade 1 or no toxicity. We observed a substantial increase in prevalence in grade 2/3 toxicities when liver doses approach 75 Gy (Table 5).

These findings are counter-intuitive to the traditional approach for dose selection and have clinical implications that (a) non-tumoral liver radiation dose may better predict treatment-related toxicity than pre-existing liver status and treatment arterial distribution, and (b) the actual dose delivered to the non-tumoral liver parenchyma can differ significantly from the uniform dose that is assumingly delivered to the treated area by current dosimetry methods. Theoretically, implementation of PET dosimetry after a treatment session may allow the operator to better plan ^{90}Y doses for repeat treatments to optimize therapy while minimizing risk of toxicity; additional studies are necessary to validate this possible clinical implication.

Limitations to this study are present. The power to better assess the baseline patient and treatment variables is limited by the relatively small number of patients. A larger study with a broader range of delivered doses would permit further refinement and validation of the statistical analyses and dose thresholds. The inclusion of both primary and secondary liver malignancies can affect the generalizability of these findings; for example, the patients with non-HCC malignancies were allowed to resume their chemotherapy regimen, if part of the standard of care, 4 weeks after radioembolization, which could attribute to observed toxicities during the study, although no significant correlation was found between toxicity and patients with non-HCC tumors. Given the fewer number of patients with secondary liver malignancies, our findings are more reflective of patients with HCC. There were few observations of grade 3 or higher toxicity, which limits the ability to further distinguish between moderate and higher toxicities grades. The majority of the treatments were also performed by lobar distribution; while this reflects a common practice at the time of this study, findings may be different with predominant use of superselective (e.g. radiation segmentectomy) or whole-liver treatment. Furthermore, the findings may differ with patients treated with resin microspheres. While these stated limitations indicate the overall heterogeneity of the study population, this study was intended to represent the diversity of actual practices by including patients with both HCC and non-HCC tumors, variations in

treatment (glass and resin microspheres, and segmental versus lobar infusions), with ^{90}Y dose selection and administration in accordance with accepted standard of care. Finally, long-term (i.e. 12 month) toxicity was not assessed in this study, and therefore instances of eventual radiation fibrosis may not be adequately captured. However, a long-term toxicity assessment is confounded by numerous factors, such as repeat/additional therapy, liver transplantation, and progression of cirrhosis. Therefore, a 120-day cutoff for toxicity analysis was chosen.

In conclusion, ^{90}Y delivered dose to normal liver parenchyma can be measured by internal pair-production PET after radioembolization of unresectable liver tumors and predicts post-treatment liver toxicity. Non-tumoral liver dose is strongly correlated to a composite of grade 2 toxicity, as well as moderate or greater laboratory changes in bilirubin and AST, with a D_{50} threshold of 54 Gy. PET dosimetry may eventually permit adjustments in dosimetry in order to further improve the safety of radioembolization. Further investigation using PET dosimetry is needed to provide additional insight into treatment-related toxicities associated with ^{90}Y radioembolization.

Acknowledgements Grants for this study: Philips Healthcare. IRB statement: This study was performed under IRB approval at the University of Washington.

Compliance with Ethical Standards

Conflict of interest S. Padia: Consultant for BTG International and the other authors have no conflicts of interest.

Ethical Approval All procedures performed in studies involving human participants were in accordance with the ethical standards of the institutional and/or national research committee and with the 1964 Helsinki declaration and its later amendments or comparable ethical standards.

Informed Consent Informed consent was obtained from all individual participants included in the study.

References

- Dancey JE, Shepherd FA, Paul K, et al. Treatment of nonresectable hepatocellular carcinoma with intrahepatic ^{90}Y -microspheres. *J Nucl Med.* 2000;41:1673–81.
- Garin E, Rolland Y, Edeline J, et al. Personalized dosimetry and intensification concept with ^{90}Y -loaded glass microsphere radioembolization induce prolonged overall survival in hepatocellular carcinoma patients with portal vein thrombosis. *J Nucl Med.* 2015;56:339–46.
- Song YS, Paeng JC, Kim HC, et al. PET/CT-based dosimetry in ^{90}Y -microsphere selective internal radiation therapy: single cohort comparison with pretreatment planning on (99m)Tc-MAA imaging and correlation with treatment efficacy. *Medicine.* 2015;94(23):e945.
- Gil-Alzugaray B, Chopitea A, Iñárraigui M, et al. Prognostic factors and prevention of radioembolization-induced liver disease. *Hepatology.* 2013;57:1078–87.
- Riaz A, Lewandowski RJ, Kulik LM, et al. Complications following radioembolization with yttrium-90 microspheres: a comprehensive literature review. *J Vasc Interv Radiol.* 2009;20:1121–30.
- Piana PE, Gonsalves CF, Sato T, et al. Toxicities after radioembolization with yttrium-90 SIR-Spheres: incidence and contributing risk factors at a single center. *J Vasc Interv Radiol.* 2011;22:1373–9.
- Lam MG, Abdelmaksoud MH, Chang DT, et al. Safety of ^{90}Y radioembolization in patients who have undergone previous external beam radiation therapy. *Int J Radiat Oncol Biol Phys.* 2013;87(2):323–9.
- Gabrielson A, Miller A, Banovac F, Kim A, He AR, Unger K. Outcomes and predictors of toxicity after selective internal radiation therapy using yttrium-90 resin microspheres for unresectable hepatocellular carcinoma. *Front Oncol.* 2015;5:292.
- Son SH, Jang HS, Jo IY, et al. Significance of an increase in the Child–Pugh score after radiotherapy in patients with unresectable hepatocellular carcinoma. *Radiat Oncol.* 2014;9:101.
- Young JY, Rhee TK, Atassi B, et al. Radiation dose limits and liver toxicities resulting from multiple yttrium-90 radioembolization treatments for hepatocellular carcinoma. *J Vasc Interv Radiol.* 2007;18:1375–82.
- Lau WY, Leung WT, Ho S, et al. Treatment of inoperable hepatocellular carcinoma with intrahepatic arterial yttrium-90 microspheres: a phase I and II study. *Br J Cancer.* 1994;70:994–9.
- Goin JE, Salem R, Carr BI, et al. Treatment of unresectable hepatocellular carcinoma with intrahepatic yttrium 90 microspheres: factors associated with liver toxicities. *J Vasc Interv Radiol.* 2005;16:205–13.
- Elschot M, Vermolen BJ, Lam MG, Keizer B, Van den Bosch MA, De Jong HW. Quantitative comparison of PET and Bremsstrahlung SPECT for imaging the in vivo yttrium-90 microsphere distribution after liver radioembolization. *PLoS ONE.* 2013;8(2):e55742.
- Padia SA, Alessio A, Kwan SW, Lewis DJ, Vaidya S, Minoshima S. Comparison of positron emission tomography and bremsstrahlung imaging to detect particle distribution in patients undergoing yttrium-90 radioembolization for large hepatocellular carcinomas or associated portal vein thrombosis. *J Vasc Interv Radiol.* 2013;24(8):1147–53.
- Salem R, Thurston KG. Radioembolization with ^{90}Y trium microspheres: a state-of-the-art brachytherapy treatment for primary and secondary liver malignancies. Part 1: technical and methodologic considerations. *J Vasc Interv Radiol.* 2006;17:1251–78.
- Salem R, Thurston KG. Radioembolization with ^{90}Y trium microspheres: a state-of-the-art brachytherapy treatment for primary and secondary liver malignancies. Part 2: special topics. *J Vasc Interv Radiol.* 2006;17:1425–39.
- Padia SA, Kwan SW, Roudsari B, Monsky WL, Coveler A, Harris WP. Superselective yttrium-90 radioembolization for hepatocellular carcinoma yields high response rates with minimal toxicity. *J Vasc Interv Radiol.* 2014;25:1067–73.
- Lea WB, Tapp KN, Tann M, Hutchins GD, Fletcher JW, Johnson MS. Microsphere localization and dose quantification using positron emission tomography/CT following hepatic intraarterial radioembolization with yttrium-90 in patients with advanced hepatocellular carcinoma. *J Vasc Interv Radiol.* 2014;25(10):1595–603.
- Pan CC, Kavanagh BD, Dawson LA, et al. Radiation-associated liver injury. *Int J Radiat Oncol Biol Phys.* 2010;76(3 Suppl):S94–100.

20. National Cancer Institute. Common Terminology Criteria for Adverse Events v4.0. NCI, NIH, DHHS. May 29, 2009. NIH publication # 09-7473.
21. Roberson JD, McDonald AM, Baden CJ, Lin CP, Jacob R, Burnett OL. Factors associated with increased incidence of severe toxicities following yttrium-90 resin microspheres in the treatment of hepatic malignancies. *World J Gastroenterol.* 2016;22(10):3006–14.
22. Strigari L, Sciuto R, Rea S, et al. Efficacy and toxicity related to treatment of hepatocellular carcinoma with ⁹⁰Y-SIR spheres: radiobiologic considerations. *J Nucl Med.* 2010;51:1377–85.
23. Smits ML. Clinical and laboratory toxicity after intra-arterial radioembolization with ⁹⁰Y-microspheres for unresectable liver metastases. *PLoS ONE.* 2013;8(10):10.
24. Kennedy AS, McNeillie P, Dezarn WA, et al. Treatment parameters and outcome in 680 treatments of internal radiation with resin ⁹⁰Y-microspheres for unresectable hepatic tumors. *Int J Radiat Oncol Biol Phys.* 2009;74(5):1494–500.
25. Lau WY, Kennedy AS, Kim YH, et al. Patient selection and activity planning guide for selective internal radiotherapy with yttrium-90 resin microspheres. *Int J Radiat Oncol Biol Phys.* 2012;82(1):401–7.
26. Hickey R, Lewandowski RJ, Prudhomme T, et al. ⁹⁰Y radioembolization of colorectal hepatic metastases using glass microspheres: safety and survival outcomes from a 531-patient multicenter study. *J Nucl Med.* 2016;57(5):665–71.
27. Srinivas S, Natarajan N, Kuroiwa J, et al. Determination of radiation absorbed dose to primary liver tumors and normal liver tissue using post-radioembolization ⁹⁰Y PET. *Front Oncol.* 2014;13(4):255.
28. Lam MG, Louie JD, Iagaru AH, Goris ML, Sze DY. Safety of repeated yttrium-90 radioembolization. *Cardiovasc Interv Radiol.* 2013;36(5):1320–8.
29. Guha C, Kavanagh BD. Hepatic radiation toxicity: avoidance and amelioration. *Semin Radiat Oncol.* 2011;21(4):256.